Erschienen in: Nature ; 524 (2015), 7564. - S. 247-251
https://dx.doi.org/10.1038/nature14884

Crucial HSP70 co-chaperone complex unlocks metazoan protein disaggregation

Nadinath B. Nillegoda[1], Janine Kirstein[2], Anna Szlachcic[1], Mykhaylo Berynskyy[3], Antonia Stank[3,4], Florian Stengel[5], Kristin Arnsburg[2], Xuechao Gao[1], Annika Scior[2], Ruedi Aebersold[5,6], D. Lys Guilbride[1], Rebecca C. Wade[1,3,7], Richard I. Morimoto[8], Matthias P. Mayer[1] & Bernd Bukau[1]

Protein aggregates are the hallmark of stressed and ageing cells, and characterize several pathophysiological states[1,2]. Healthy metazoan cells effectively eliminate intracellular protein aggregates[3,4], indicating that efficient disaggregation and/or degradation mechanisms exist. However, metazoans lack the key heat shock protein disaggregase HSP100 of non-metazoan HSP70 dependent protein disaggregation systems[5,6], and the human HSP70 system alone, even with the crucial HSP110 nucleotide exchange factor, has poor disaggregation activity *in vitro*[4,7]. This unresolved conundrum is central to protein quality control biology. Here we show that synergic cooperation between complexed J-protein co-chaperones of classes A and B unleashes highly efficient protein disaggregation activity in human and nematode HSP70 systems. Metazoan mixed class J-protein complexes are transient, involve complementary charged regions conserved in the J-domains and carboxy-terminal domains of each J-protein class, and are flexible with respect to subunit composition. Complex formation allows J-proteins to initiate transient higher order chaperone structures involving HSP70 and interacting nucleotide exchange factors. A network of cooperative class A and B J-protein interactions therefore provides the metazoan HSP70 machinery with powerful, flexible, and finely regulatable disaggregase activity and a further level of regulation crucial for cellular protein quality control.

To investigate the possibility of a potent protein disaggregation activity in metazoans, we focused on the HSP70 chaperone system, which displays some *in vitro* capacity to disentangle and refold aggregated polypeptides when powered by an HSP110 co-chaperone[4,7]. The HSP70 J-protein HSP110 functional cycle described in Extended Data Fig. 1a, by generally accepted extrapolation, occurs on protein aggregate surfaces. Homodimeric J-proteins are essential components of this cycle[8,9]. Three classes of J-proteins (A, B and C) with >50 members in humans, determine HSP70 substrate selection, with some functional redundancy among members[9]. For example, class A and B J-proteins (Fig. 1a) implicated in protein quality control have common functions, but independent and differing efficacies[9–11]. The basis for the evolutionary maintenance of these two classes of J-proteins (despite appreciable internal diversity[12,13]), and the relation of class to function and principles governing substrate selection, remain unknown.

Here we explore the full potential of the metazoan HSP70–J-protein–HSP110 system in protein disaggregation, by examining the functional relationship between class A and B J-proteins. Using thermally denatured luciferase from *Photinus pyralis* as model substrate[4], we investigate the *in vitro* protein disaggregation/refolding versus protein refolding only (Extended Data Fig. 1b–d) capacities of the human and *Caenorhabditis elegans* HSP70–HSP110 systems (also known as HSPA8–HSPH2 in humans, and HSP-1–HSP-110 in *C. elegans*) in conjunction with class A and B J-proteins (Fig. 1, Extended Data Fig. 1e and Extended Data Table 1).

In disaggregation/refolding reactions with a class A (JA2) and B (JB1) J-protein present together (Fig. 1b, magenta), rather than either class J-protein alone (Fig. 1b, green or blue), we observed unprecedented reactivation of pre-formed heat-aggregated luciferase, indicating synergistically accelerated protein disaggregation. This was also seen under limiting chaperone concentrations (maintained in all further experiments) with multiple class A (JA1 and JA2) and class B (JB1 and JB4) human J-proteins (Extended Data Figs 1f and 2a). Disaggregation reactions with the corresponding nematode HSP-1–HSP-110 system and J-proteins DNJ-12 (class A) and DNJ-13 (class B) show similar synergic acceleration (Fig. 1c and Extended Data Fig. 2c, d). In reactions containing only one J-protein class (Extended Data Fig. 1f, JA2, solid lines; or JB1, dashed lines), with increased J-protein levels of threefold or more relative to the mixed class J-protein reaction (Extended Data Fig. 1f, magenta), protein disaggregation/refolding slows and is inhibited. We infer that the presence of class A and B J-proteins together, rather than J-protein amount, determines reaction efficiency. Both the disaggregation/refolding rate (Extended Data Fig. 2e, f) and yield (Extended Data Fig. 2g) of renatured luciferase peak with equal proportions of class A to B. A broad range of flanking reciprocal A to B J-protein stoichiometries also show appreciable activity, suggesting that efficient disaggregation/refolding is supported by minimal amounts of preferentially interacting A and B J-proteins. Increased initial rates at higher stoichiometries of JA2 (Extended Data Fig. 2f) reflect intrinsically higher refolding capacity of class A J-proteins with HSP70 (Extended Data Fig. 2b, green)[14].

Disaggregation synergy in mixed J-protein class reactions occurs with and without small HSP (*Saccharomyces cerevisiae* Hsp26) incorporation into aggregates for both human (Extended Data Figs 1f and 3a) and nematode J-protein containing systems (Fig. 1c and Extended Data Fig. 2d). Synergy is independent of nucleotide exchange factors (NEFs) (Extended Data Fig. 3b), protein substrate (Fig. 1b and Extended Data Fig. 3c, d) and substrate concentration variations affecting density, size[4] and therefore the architectural nature of the aggregate generated (Extended Data Fig. 3e). Synergy also occurs at lower chaperone to substrate ratios (Fig. 1b and Extended Data Figs 1f and 3f), and at different and characteristic ranges of substrate to J-protein ratio for malate dehydrogenase (MDH) versus luciferase or α-glucosidase disaggregation (Fig. 1b and Extended Data Fig. 3c, d). MDH aggregates resolve considerably with non-limiting concentrations of JB1 alone (not shown), but with limiting JB1 concentrations in the presence of JA2, synergic MDH disaggregation occurs (Extended Data Fig. 3d). Synergy in disaggregation therefore appears generic, operating over a range of ratios and concentrations, with room for substrate-linked variation. By contrast, refolding only reactions show

[1]Center for Molecular Biology of the University of Heidelberg (ZMBH), German Cancer Research Center (DKFZ), DKFZ-ZMBH Alliance, 69120 Heidelberg, Germany. [2]Leibniz-Institute for Molecular Pharmacology (FMP), 13125 Berlin, Germany. [3]Heidelberg Institute for Theoretical Studies (HITS), 69118 Heidelberg, Germany. [4]Heidelberg Graduate School of Mathematical and Computational Methods for the Sciences, Heidelberg University, 69120 Heidelberg, Germany. [5]Department of Biology, Institute of Molecular Systems Biology, ETH Zurich, 8093 Zurich, Switzerland. [6]Faculty of Science, University of Zurich, 8057 Zurich, Switzerland. [7]Interdisciplinary Center for Scientific Computing (IWR), Heidelberg University, 69120 Heidelberg, Germany. [8]Department of Molecular Biosciences, Rice Institute for Biomedical Research, Northwestern University, Evanston, Illinois 60208, USA.

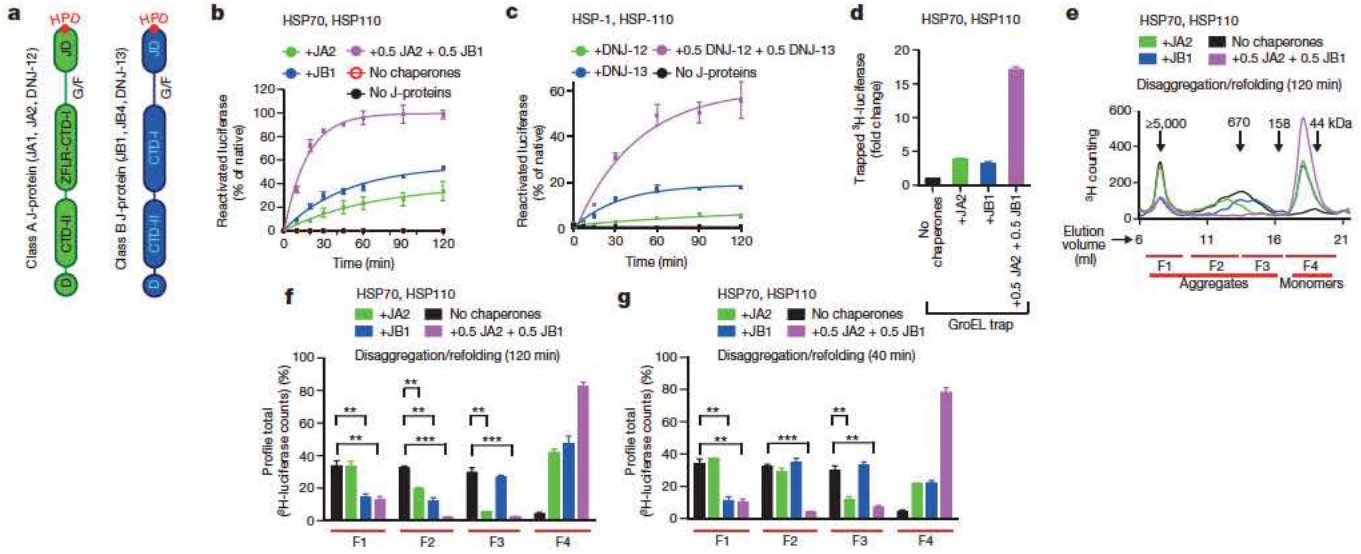

Figure 1 | Simultaneous presence of class A and B J proteins unleashes protein disaggregation activity and broadens target aggregate range of the HSP70 machinery. **a**, Two distinct classes (A and B) display highly conserved domain organization involving the HSP70 intertacting HPD motif (red) containing amino terminal J domain (JD), Gly/Phe rich flexible region (G/F), C terminal β sandwich domains (CTD I and II), with class A J proteins distinguished mainly by a zinc finger like region (ZFLR) that inserts into the CTD I subdomain and a dimerization domain (D)[9,23]. CTD together with ZFLR provide substrate specificity[24,25]. **b**, Disaggregation and reactivation of preformed luciferase aggregates using human HSP70 HSP110 with human J proteins JA2 (green), JB1 (blue), JA2+JB1 (magenta) or with no J proteins (black) ($n = 3$). **c**, Reactivation of heat aggregated luciferase by nematode HSP70 machinery containing HSP 1, HSP 110 and either alone or in combination with the nematode J proteins DNJ 12 (A) and DNJ 13 (B) ($n = 2$). **d**, Fold change in trapped luciferase; control, GroEL^{D87K} without other chaperones (black). Values normalized to total ^{3}H counts in each reaction ($n = 2$). **e**, SEC profile after disaggregation/refolding (120 min) with either J protein alone or combined. Elution fractions labelled F1 F4 (red lines); F4, disaggregated monomers (~63 kDa). **f**, Aggregate quantification for fractions F1 F4 from the SEC profile in e. Disappearance of ^{3}H luciferase from aggregates (F1 F3) occurs with concomitant accumulation of disaggregated monomer (F4). **g**, Aggregate quantification, after 40 min disaggregation. Values normalized to total counts in each reaction. Two tailed t test, $^{**}P < 0.01$, $^{***}P < 0.001$ ($n = 3$). Data are mean ± s.e.m. Precise concentrations are shown in Extended Data Table 1.

no synergism (Extended Data Fig. 2b). We conclude that efficient protein disaggregation, but not refolding, requires cooperation between class A and B J proteins.

Three non exclusive mechanisms could explain the synergistic action of class A and B J proteins. In a mechanism involving sequential action, one J protein class interacts with HSP70 HSP110 to extract polypeptides from aggregates. The other J protein class then prevents re aggregation of extracted polypeptide (holdase function) and/or in combination with HSP70 HSP110 promotes substrate refolding. Of the four J proteins tested for holdase function, only JA2 and JB4 prevent luciferase aggrega tion at 42 °C (Extended Data Fig. 3g, h). However, disaggregation synergy is indistinguishable for J protein combinations with (JA2 or JB4) and without (JA1 or JB1) holdase function (Extended Data Fig. 2a). Furthermore, disaggregation/refolding rates are unaffected by the order of JA2 and JB1 addition during the reaction (Extended Data Fig. 3i), indicating that J proteins act in no strict order. For direct validation, we quantified tritium labelled luciferase extracted from aggregates using a mutant GroEL protein (GroEL^{D87K}) as a trap[15] for extracted luciferase molecules, preventing refolding. Decreased luciferase activity in disag gregation/refolding reactions in the presence of GroEL^{D87K} reflects trap ping of labelled disaggregated polypeptides (Extended Data Fig. 4a, b), counted by measuring tritium scintillation (Fig. 1d). Disaggregation/ refolding reactions containing only one class of J protein show similar amounts of trapped ^{3}H labelled luciferase polypeptides. With class A and B J proteins present together, however, we see synergistically accelerated accumulation of disaggregated ^{3}H labelled luciferase trapped in GroEL (Fig. 1d). Together, these results exclude a strictly sequential function of J protein classes in disaggregation/refolding, corroborating the inference that synergy occurs at the protein disaggregation step.

A second model stipulates that each J protein class acts specifically, in parallel, distinguishing protein aggregates by size and/or compact ness during the disaggregation step. We tested this by adding different J protein HSP70 HSP110 mixtures to preformed ^{3}H labelled lucifer ase aggregates, which display a range of sizes, and probably variations in molecular architecture. We analysed the disaggregation of aggregate populations by size exclusion chromatography (SEC; Fig. 1e g and Extended Data Fig. 4c, d). Reactions were run in parallel, stopped by depleting ATP with apyrase, and held on ice until SEC (Extended Data Fig. 4e). Eluted fractions (F1 F4, Fig. 1e g) reveal JA2 containing chaperone mixes preferentially solubilize smaller aggregates (F3; ~200 700 kilodaltons (kDa)). Conversely, JB1 containing mixes preferentially solubilize larger aggregates (F1, ≥5,000 kDa; F2, ~700 4,000 kDa), but solubilize small aggregates less efficiently. These results are consistent with distinct, parallel class activity. JA2 plus JB1 combinations, however, in much shorter reactions (40 min instead of 120 min), solubilize both larger and smaller aggregates far more efficiently than the added efficiencies of separate JA2 and JB1 reactions allow (Fig. 1g). Similar results obtain throughout for α glucosidase aggregate solubilization (Extended Data Fig. 4d). This suggests concerted action on the same target.

This prompts a third model, in which synergy results from the formation of mixed class J protein complexes exerting concerted activity to facilitate disaggregation. A range of approaches rigorously tests this model.

To visualize individual versus complexed J protein function, we biased disaggregation/refolding reactions by combining JA2:JB1 in 5:1 to 1:5 ratios, then analysed aggregate resolution by SEC (Extended Data Fig. 4f). The 1:1 ratios dissolve all aggregates (F1 F3, magenta). In con trast, limiting JB1 concentration and excess JA2 in shorter reactions (40 min, orange solid) barely resolves the largest aggregates (F1), whereas the smaller aggregates (F2 F3) disappear completely; F1 aggregates resolve only in longer reactions (120 min, orange hash). Limiting JB1 concentrations alone, however, readily resolve large F1 aggregates (blue solid). We infer that scarce JB1 molecules preferentially sequester with excess JA2 into complexes that efficiently process all sizes of aggregates; the smaller F2 and F3 aggregates accordingly disappear first. Reciprocal titration with scarce JA2 and excess JB1 concentration shows less dis aggregation of the smaller F2 and F3 aggregates (magenta versus red

solid, Extended Data Fig. 4f), which fully resolve with a longer reaction time (120 min, red hash). Specific J protein stoichiometries evidently modulate HSP70 targeting and disaggregation efficacy. We infer that J proteins preferentially form efficient mixed class complexes, supporting a model for concerted action.

Independent tests for physical interactions between class A and B J proteins consistently reveal intermolecular J domain C terminal domain (JD CTD) and CTD CTD contacts. Approaches include chemical cross linking coupled to mass spectrometry (Fig. 2a), Förster resonance energy transfer (FRET; Fig. 2b), docking simulations (Fig. 2c, d) and competition assays (Fig. 2e).

Mass spectrometry of JA2 and JB1 combinations treated with lysine specific cross linker (disuccinimidyl suberate) identifies three intermolecular cross linked regions between JD^{JA2} CTD^{JB1}, JD^{JB1} CTD^{JA2} and CTD^{JA2} CTD^{JB1} (Fig. 2a and Extended Data Fig. 5a, b). FRET measured by donor quenching indicates JD CTD and CTD CTD interactions between JA2 and JB1 in solution (Fig. 2b, J protein pairs 1, 2 and 3; Extended Data Fig. 6a). This corroborates our cross linking data and favours biological relevance. We detect neither JD JD interactions between classes (J protein pair 4), nor intermolecular same class JD CTD interactions (J protein pair 5). However, in agreement with structures from small angle X ray scattering of class B J proteins[16,17], we detect JD^{JB1} CTD^{JB1} cross links (not shown). Presumably these reflect intramolecular interactions, preventing intermolecular JD^{JB1} CTD^{JB1} but not JD^{JA2} CTD^{JB1} interactions, as indicated by FRET (Fig. 2b).

We further defined the interface of the JA2 JB1 complex using unbiased docking simulations between J domain and CTD dimers of JA1, JA2, JB1 and JB4 (Fig. 2c, d and Extended Data Fig. 7a, b). Simulations show a preferred binding arrangement of JD^{JB1} on CTD^{JA2} and conversely JD^{JA2} on CTD^{JB1} (Fig. 2c, d), again corroborating cross linking data (Fig. 2a).

Furthermore, in competition experiments, the addition of moderate excess of isolated J domain fragments inhibits JA2 JB1 HSP70 HSP110 dependent disaggregation/refolding of heat aggregated luciferase (Fig. 2e), although not refolding alone (Fig. 2f). J domain fragments carrying the HPD motif mutated to QPN, which abolishes the JD HSP70 interaction and ATP hydrolysis stimulation on HSP70 (refs 18, 19), have the same effect (Extended Data Fig. 6e), confirming that inhibition of disaggregation is not due to HSP70 being titrated out by J domain fragment binding. Unlabelled full length J proteins and isolated J domains compete with mixed class JD CTD interactions, indicated by decreased FRET efficiency between JA2 and JB1 (Extended Data Fig. 6f, g), explaining the inhibitory effects. However, JD CTD interaction sites do not overlap CTD binding sites for substrate, since JA2 holdase activity remains unaffected with isolated J domains present (Extended Data Fig. 7c, d). Molecular docking modelling supports this also (Extended Data Fig. 8). J protein complexing involving mixed class J domains and CTDs is therefore crucial for efficient protein disaggregation, but not for refolding.

Non ionic detergent affects neither disaggregation activity (Extended Data Fig. 6b) nor FRET efficiency between class A and B molecules (Extended Data Fig. 6a). Increasing salt concentrations, however, weaken both (Extended Data Fig. 6c, d), suggesting ionic interactions. Independent methodologies therefore confirm specific JD CTD interactions of a predominantly electrostatic nature directly implicated in disaggregation efficiency.

J domain and CTD regions display highly conserved, class specific electrostatic potentials (Fig. 3a, b). Class A J proteins show distinct polarity in the CTDs, with negatively charged regions (red) in the CTD II and dimerization subdomains, and positively charged regions (cyan) along the zinc finger like region and CTD I hook (Fig. 3a). Conversely, class B CTDs are relatively non polar, with positively charged regions in the CTD where JD^{JA2} cross linking occurs. J domains in both classes are markedly bipolar, although class A J domains have smaller negatively charged regions (Fig. 3b). In all J domains, positive charge (near the HPD motif and helix II) is implicated in binding to HSP70 (refs 18, 19). We deduce conserved negatively charged regions exposed in the J domains interact with positively charged CTD regions in opposite class J proteins.

We therefore generated triple charge reversal variants of the J domain ($JA2^{RRR}$ or $JB1^{RRR}$), replacing negatively charged Asp or Glu residues with positively charged Arg residues in and around helices I and IV (Fig. 3c). FRET interactions between the JD^{JA2} and CTD^{JB1} regions diminish with charge reversal mutations in either JD^{JA2} or JD^{JB1} (Fig. 3d, J protein pairs 2 and 3), and are abrogated with charge reversals in both interacting J domains (Fig. 3d, J protein pair 4). Partial FRET reduction with triple charge reversals in only one interacting JD CTD domain pair suggests some degree of intermolecular tethering by the other pair, although insufficient for full J protein cooperation and disaggregation efficiency (Fig. 3e). In refolding only reactions, recovered luciferase activity remains unaffected by J domain charge reversals (Fig. 3f). Physically complexed and cooperating mixed class J proteins are therefore essential for efficient HSP70 dependent disaggregase activity, and are thought (but not directly shown) to act on the surface of

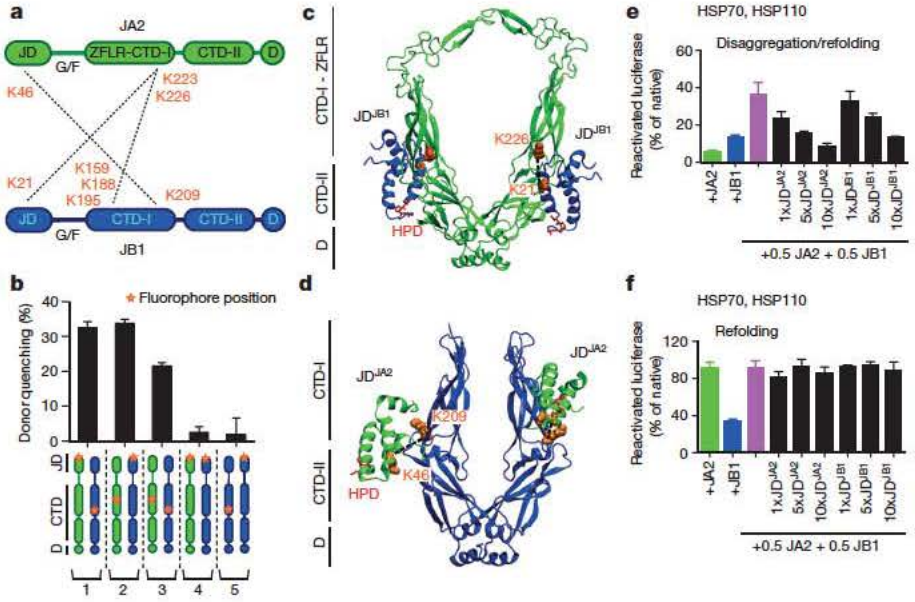

Figure 2 | Intermolecular JD CTD interaction is required for mixed class J protein complex formation. **a**, Intermolecular cross links (dashed lines) between Lys residues (orange) on JA2 (green) and JB1 (blue). **b**, JA2 and JB1 interactions analysed by FRET. Bars show donor quenching efficiency of JD CTD interactions; cartoons below show fluorophore positions in J protein protomer pairs 1–5. N termini of JD^{JA2} and JD^{JB1} are labelled with acceptor fluorophore ReAsH. CTD^{JA2} and CTD^{JB1} are labelled with donor fluorophores FlAsH and Alexa Fluor 488 at residues 241 and 278, respectively ($n = 3$). **c**, **d**, Ribbon diagrams showing representative positions of JDs on CTD dimers from docking simulations; cross linked Lys residues (space filling, orange, connected with black dashed lines) established in a; HPD motif (stick representation, red). **c**, JD^{JB1} (blue) and CTD^{JA2} (green). **d**, JD^{JA2} (green) and CTD^{JB1} (blue). **e**, **f**, Competition of excess isolated JD fragments for classes A and B J protein complex formation and effect on luciferase disaggregation. **e**, **f**, Protein disaggregation/refolding (**e**) and refolding only (**f**) ($n = 3$). Data are mean ± s.e.m. Precise concentrations are shown in Extended Data Table 1.

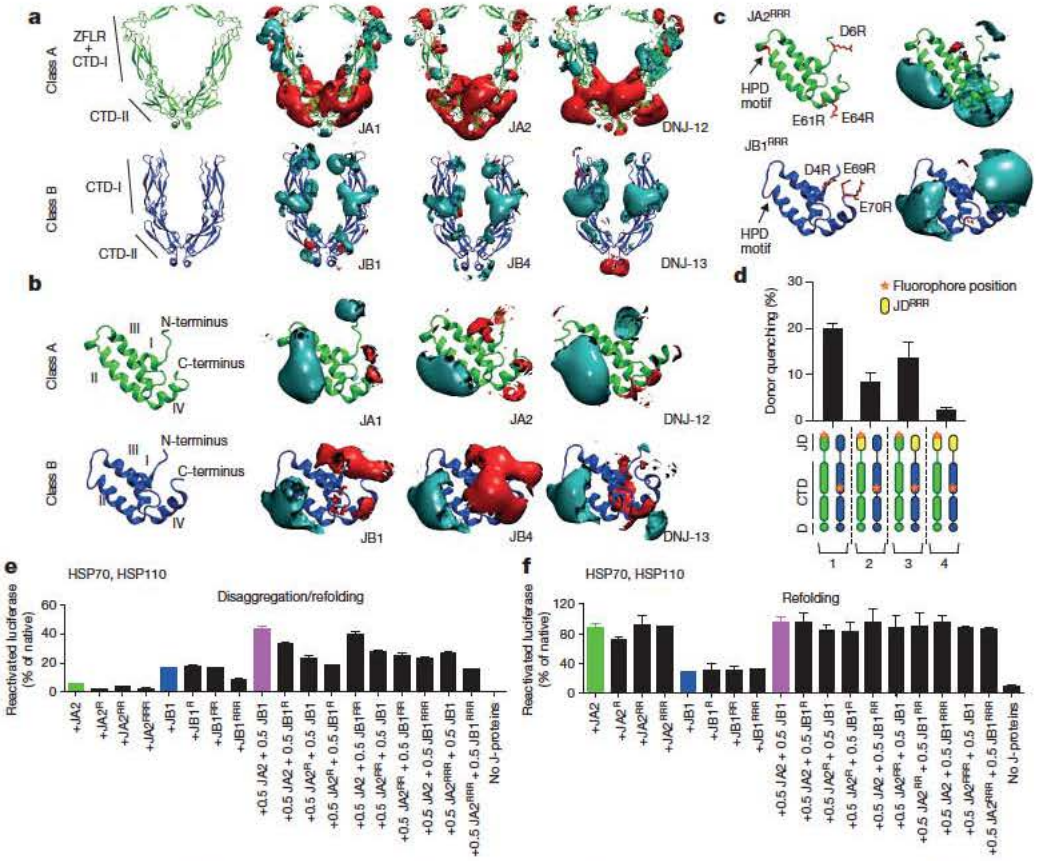

Figure 3 | Conserved electrostatic potential distributions in A and B J protein classes are complementary and direct mixed class J protein interactions for complex formation. **a**, Electrostatic isopotential maps of CTD dimers comparing human (JA1, JA2, JB1 and JB4) and nematode (DNJ 12 and DNJ 13) class A and B J proteins. Electrostatic potential around proteins is contoured at +1 (positive, cyan) and −1 (negative, red), kcal mol $^{1}e^{1}$. Protein structures are represented by ribbon diagrams. **b**, Conserved α helices and electrostatic isopotential maps contoured as in a of human and nematode J domains. I IV (from N terminus) denote conserved α helices. **c**, The J domains of charge reversal triple mutants (JA2^{RRR} and JB1^{RRR}); and their electrostatic isopotential maps compare with wild types in **b**. RRR denotes triple amino acid substitutions D6R, E61R and E64R in JA2, and D4R, E69R and E70R in JB1. **d**, FRET determination of JA2 and JB1 triple charge reversa; mutants ($n = 3$). Bars show donor quenching efficiency of JD CTD interactions; cartoons below show fluorophore positions in J protein protomer pairs 1 4. Triple charge mutants are yellow. **e**, Luciferase disaggregation/refolding at 120 min with J domain charge reversal mutants (JA2: D6R (R); E61R+E64R (RR); D6R+E61R+E64R (RRR). JB1: D4R (R); E69R+E70R (RR); D4R+E69R+E70R (RRR)) ($n = 3$). **f**, As in **e**, refolding only at 80 min ($n = 3$). Data are mean ± s.e.m. Precise concentrations are shown in Extended Data Table 1.

aggregates. A paradoxical sequence dispensability of these highly con served helices I and IV observed in early data, which assayed exclu sively for HSP70 interaction and protein folding[18,20], is also now explained. These data together strongly support a mixed class J protein interaction with vital function conserved in evolution.

Size separation of tritiated JB1 mixed with unlabelled, larger JA2, or the reciprocal labelling, reveals only JB1 (blue) or JA2 (green) homo dimers (Extended Data Fig. 5c), indicating that J protein complexes are transient. Transient interactions would support an HSP70 disaggregation machinery with a flexible range of tailored activities. Single class J protein function shows HSP70 HSP110 mediated dis aggregation activity limited to aggregates of specific size ranges (Fig. 4, large or small aggregates). Mixed class J protein complexes efficiently disaggregate a wide range of aggregate sizes (Fig. 4, large, medium and

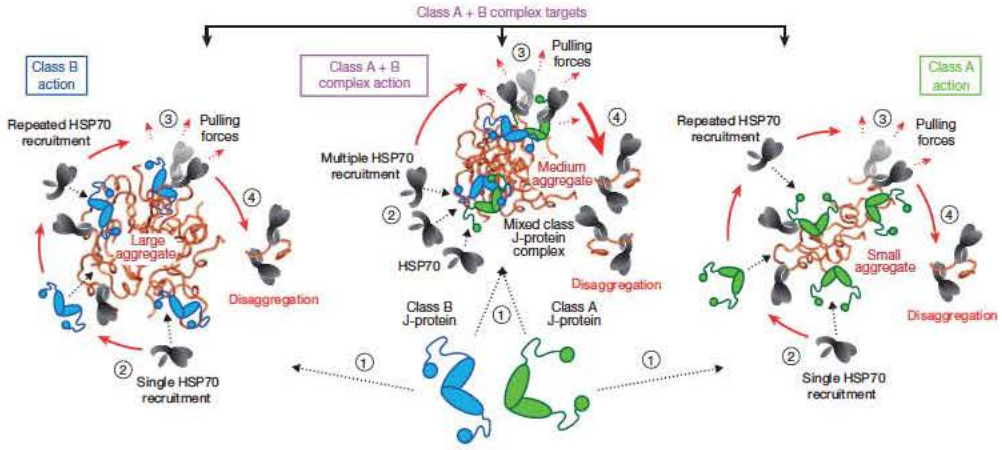

Figure 4 | Model of individual versus complexed class A and class B J protein function in protein disaggregation. Size specific aggregate targeting: large aggregates are targeted by J protein$^{class\ B}$ HSP70 HSP110 (blue); small aggregates are targeted by J protein$^{class\ A}$ HSP70 HSP110 (green); all aggregates sizes are targeted by J protein mixed class complex HSP70 HSP110 (magenta). HSP70 molecules are in grey. Sequential reaction steps (encircled numbers): 1, J protein targets aggregate; 2, J protein recruits HSP70; 3, surface bound chaperones generate pulling forces (dashed red arrows); and 4, polypeptide extraction leading to protein disaggregation. Chaperone recruitment denoted by dashed black arrows.

small). On the basis of our results, we reason a minimum complex consists of one class A J protein homodimer binding to one class B homodimer in a 1:1 ratio, indicating that there are four J domains per complex. Assuming two J domains engage in interactions sufficient to complex the J proteins, one J domain per homodimer remains free to interact with one HSP70, allowing for recruitment of two interacting HSP70 molecules per complex without steric hindrance (Fig. 4, med ium aggregates, Extended Data Fig. 8). We conclude that each mixed class J protein complex recruits at least two HSP70 molecules per targeting event, possibly seeding dynamic, higher order chaperone assemblies on aggregate surfaces.

Our computational models of the structures of mixed class J protein complexes (Extended Data Fig. 8) incorporate the constraints defined by all our cross linking, FRET and docking data. In each model, space in the J protein complex allows for substrate binding via several interfaces, HSP70 interaction with J domains, and HSP110 interaction with each HSP70 protein. These models accommodate the concept of entropic pulling, in which HSP70 binding to entangled polypeptides decreases entropy, generating reciprocal forces that pull polypeptides from aggre gates[21]. Such higher order chaperone complexes would be expected to increase pulling forces and stabilize disaggregating polypeptides by pro viding increased substrate binding surface, thereby accelerating protein disaggregation (Fig. 4; class A+B complex). Although also likely, direct verification of mixed class J protein HSP70 complexes interspersed with single class J protein HSP70 complexes on aggregate surfaces is currently experimentally intractable.

In summary, we demonstrate potent protein disaggregation activity in metazoans, mediated by the central HSP70 J protein HSP110 chaper one network. Disaggregation efficacy comparable to that of non meta zoan HSP100 HSP70 bi chaperone systems, over a broad aggregate size range, requires transient physical interaction between class A and B J proteins. The assembly of higher order chaperone complexes on pro tein aggregate surfaces is expected to increase coordinated pulling forces on multiple trapped polypeptides, providing a plausible mechanistic basis for increased disaggregation efficacy. Mixed class J protein com plexes form preferentially and interact with HSP70 HSP110 to resolve a broad range of aggregates efficiently, whereas single class J protein HSP70 HSP110 interaction targets specific aggregate sizes. This suggests intracellular J protein stoichiometry will differentially regulate HSP70 dependent protein disaggregation efficiency. The transitory nature of J protein complexes would, in this context, facilitate flexible response according to need. As in nematodes, human cytosol contains several members of J protein classes: four class A and nine class B J proteins[9]. A wide range of complexed J protein combinations is therefore available in humans and other metazoa, providing flexible target selectivity. This opens the further possibility of physiological function in assembly/dis assembly of other macromolecular cell structures. These findings may also impinge on the amorphous, oligomeric, most toxic prefibrilar phase of amyloidic fibre formation characterizing neurodegenerative diseases[22]. Overall, our work identifies a physically interacting J protein network that adds another level of functional flexibility to cellular protein quality control. The underlying functional basis for hitherto unexplained evolu tionary maintenance of distinct J protein classes now also becomes clear. In essence, we reveal a J protein gearbox regulating efficacy of protein disaggregation and consequently, refolding reactions, with fundamental effect on the cellular physiology, and therefore health, of metazoan organisms.

1. Hipp, M. S., Park, S. H. & Hartl, F. U. Proteostasis impairment in protein misfolding and aggregation diseases. *Trends Cell Biol.* **24,** 506 514 (2014).
2. Morimoto, R. I. Proteotoxic stress and inducible chaperone networks in neurodegenerative disease and aging. *Genes Dev.* **22,** 1427 1438 (2008).
3. Kirstein Miles, J., Scior, A., Deuerling, E. & Morimoto, R. I. The nascent polypeptide associated complex is a key regulator of proteostasis. *EMBO J.* **32,** 1451 1468 (2013).
4. Rampelt, H. *et al.* Metazoan Hsp70 machines use Hsp110 to power protein disaggregation. *EMBO J.* **31,** 4221 4235 (2012).
5. Goloubinoff, P., Mogk, A., Zvi, A. P., Tomoyasu, T. & Bukau, B. Sequential mechanism of solubilization and refolding of stable protein aggregates by a bichaperone network. *Proc. Natl Acad. Sci. USA* **96,** 13732 13737 (1999).
6. Parsell, D. A., Kowal, A. S., Singer, M. A. & Lindquist, S. Protein disaggregation mediated by heat shock protein HSP104. *Nature* **372,** 475 478 (1994).
7. Shorter, J. The mammalian disaggregase machinery: Hsp110 synergizes with Hsp70 and Hsp40 to catalyze protein disaggregation and reactivation in a cell free system. *PLoS ONE* **6,** e26319 (2011).
8. Mayer, M. P. & Bukau, B. Hsp70 chaperones: cellular functions and molecular mechanism. *Cell. Mol. Life Sci.* **62,** 670 684 (2005).
9. Kampinga, H. H. & Craig, E. A. The HSP70 chaperone machinery: J proteins as drivers of functional specificity. *Nature Rev. Mol. Cell Biol.* **11,** 579 592 (2010).
10. Cyr, D. M. & Ramos, C. H. Specification of Hsp70 function by type I and type II HSP40. *Subcell. Biochem.* **78,** 91 102 (2015).
11. Sahi, C. & Craig, E. A. Network of general and specialty J protein chaperones of the yeast cytosol. *Proc. Natl Acad. Sci. USA* **104,** 7163 7168 (2007).
12. Tzankov, S., Wong, M. J., Shi, K., Nassif, C. & Young, J. C. Functional divergence between co chaperones of Hsc70. *J. Biol. Chem.* **283,** 27100 27109 (2008).
13. Rauch, J. N. & Gestwicki, J. E. Binding of human nucleotide exchange factors to heat shock protein 70 (Hsp70) generates functionally distinct complexes *in vitro*. *J. Biol. Chem.* **289,** 1402 1414 (2014).
14. Lu, Z. & Cyr, D. M. Protein folding activity of HSP70 is modified differentially by the Hsp40 co chaperones Sis1 and Ydj1. *J. Biol. Chem.* **273,** 27824 27830 (1998).
15. Weibezahn, J. *et al.* Thermotolerance requires refolding of aggregated proteins by substrate translocation through the central pore of ClpB. *Cell* **119,** 653 665 (2004).
16. Ramos, C. H., Oliveira, C. L., Fan, C. Y., Torriani, I. L. & Cyr, D. M. Conserved central domains control the quaternary structure of type I and type II HSP40 molecular chaperones. *J. Mol. Biol.* **383,** 155 166 (2008).
17. Borges, J. C., Fischer, H., Craievich, A. F. & Ramos, C. H. Low resolution structural study of two human HSP40 chaperones in solution. DJA1 from subfamily A and DJB4 from subfamily B have different quaternary structures. *J. Biol. Chem.* **280,** 13671 13681 (2005).
18. Tsai, J. & Douglas, M. G. A conserved HPD sequence of the J domain is necessary for YDJ1 stimulation of Hsp70 ATPase activity at a site distinct from substrate binding. *J. Biol. Chem.* **271,** 9347 9354 (1996).
19. Suh, W. C., Lu, C. Z. & Gross, C. A. Structural features required for the interaction of the Hsp70 molecular chaperone DnaK with its cochaperone DnaJ. *J. Biol. Chem.* **274,** 30534 30539 (1999).
20. Genevaux, P., Schwager, F., Georgopoulos, C. & Kelley, W. L. Scanning mutagenesis identifies amino acid residues essential for the *in vivo* activity of the *Escherichia coli* DnaJ (Hsp40) J domain. *Genetics* **162,** 1045 1053 (2002).
21. De Los Rios, P., Ben Zvi, A., Slutsky, O., Azem, A. & Goloubinoff, P. Hsp70 chaperones accelerate protein translocation and the unfolding of stable protein aggregates by entropic pulling. *Proc. Natl Acad. Sci. USA* **103,** 6166 6171 (2006).
22. Caughey, B. & Lansbury, P. T. Protofibrils, pores, fibrils, and neurodegeneration: separating the responsible protein aggregates from the innocent bystanders. *Annu. Rev. Neurosci.* **26,** 267 298 (2003).
23. Cheetham, M. E. & Caplan, A. J. Structure, function and evolution of DnaJ: conservation and adaptation of chaperone function. *Cell Stress Chaperones* **3,** 28 36 (1998).
24. Li, J., Qian, X. & Sha, B. The crystal structure of the yeast Hsp40 Ydj1 complexed with its peptide substrate. *Structure* **11,** 1475 1483 (2003).
25. Lu, Z. & Cyr, D. M. The conserved carboxyl terminus and zinc finger like domain of the co chaperone Ydj1 assist Hsp70 in protein folding. *J. Biol. Chem.* **273,** 5970 5978 (1998).

Acknowledgements We thank A. Mogk for critical reading of the manuscript and S. Ungelenk for Hsp26. This work was funded by the Deutsche Forschungsgemeinschaft (SFB1036, BU617/19 1 to B.B.; EXC257, SFB740 to J.K.), Alexander von Humboldt Foundation Postdoctoral Fellowships (to N.B.N. and A.Sz.), National Institutes of Health (the NIGMS, NIA, NIMS), Ellison Medical Foundation and Daniel F. and Ada L. Rice Foundation (to R.I.M.), German Federal Ministry of Education and Research (BMBF) Virtual Liver Network and EU FEP Flagship Programme Human Brain Project (0315749, 604102 to R.C.W.), Klaus Tschira Foundation (to M.B., A.St. and R.C.W.), Sir Henry Wellcome Postdoctoral Fellowship (to F.S.), ETH Zurich and ERC advanced grant Proteomics v3.0 (233226 to R.A.).

Author Contributions N.B.N. and B.B. conceived the study. N.B.N., J.K., A.Sz., M.B., A.St., F.S., D.L.G., R.C.W., M.P.M. and B.B. designed the experiments. N.B.N., J.K., A.Sz., M.B., A.St., F.S., K.A., X.G. and A.Sc. performed the experiments. N.B.N., J.K., A.Sz., M.B., A.St., F.S., R.A., R.C.W., R.I.M., D.L.G., M.P.M. and B.B. analysed the data. N.B.N., D.L.G., M.P.M. and B.B. wrote the manuscript.

Author Information Reprints and permissions information is available at www.nature.com/reprints. The authors declare no competing financial interests. Readers are welcome to comment on the online version of the paper. Correspondence and requests for materials should be addressed to B.B. (bukau@zmbh.uni heidelberg.de) or N.B.N. (n.nillegoda@zmbh.uni heidelberg.de).